

**Paul Williams, Xie Shao, and Keith Strassner, "The Contributions of Organic Anti-reflective Coatings in Modern Optical Lithography," *SEMICON China 2001 SEMI Technical Symposium*, March 28-29, 2001, pp. G-1 – G-7.**

As presented at the SEMICON China 2001 SEMI Technical Symposium on March 28-29, 2001, in the China World Hotel, Beijing, China.

# The Contributions of Organic Anti-reflective Coatings in Modern Optical Lithography

Paul Williams, Xie Shao and Keith Strassner  
Brewer Science, Inc.,  
2401 Brewer Drive, Rolla, MO 65401, USA

## Biography

*Paul Williams received his B.S in Physics from Nottingham University in 1989 and his Ph.D. on hot electron transport in GaAs devices from University of Wales, Cardiff in 1993. Before joining BSL as an application engineer, he worked as a Postdoctoral Research Associate at Cavendish Laboratories of Cambridge University on laser spectroscopy of GaAs devices. His current position is marketing manager in Asia.*

*Xie Shao received her Ph. D. in organic chemistry from the University of Basel, Switzerland, followed by two years postdoctoral experience in Ciba-Geigy AG, Department of Pharmaceutical research, and one year postdoctoral in SUNY (State University of New York) at Buffalo, Department of medicinal chemistry. She joined Brewer Science in 1993 as Sr. Research Associate. Her current position is the Manager of Anti-reflective coating's group in the R&D division, Brewer Science Inc.*

*Keith Strassner received a Master Degree in Marketing from Webster University and a BS Chemistry degree from the University of Missouri-Rolla. He joined Brewer Science in 1998 as Manager of Global Marketing, ARC Division having served in a variety of marketing and business development functions in the specialty chemical industry.*

## Abstract:

The implementation of a spin on organic anti-reflective coating (BARC) has been shown to minimize critical dimension (CD) distribution by reducing dispersive effects. These effects originate from refractive index differences between the air and photoresist, the photoresist and substrate and also incoupling within the resist commonly referred to as thin film interference [TFI]. Proximity effects such as reflective notching also introduce undesirable exposure [on positive resists] further increasing CD variation. In addition, with the advent of chemically amplified photoresist systems, more attention has been given to chemical interactions between the resist and substrate and also between the substrate and resist. These interactions can result in T-topping and footing within the resist flank, which also contribute to CD dispersion. This

paper will review the more common problems to which BARC processes are applied and the challenges associated with their integration into manufacturing. This article will also review the chemical properties of common BARCs.

**Keywords:** Optical lithography, Anti-reflective coating, CD control, Exposure latitude, Focus latitude.

## 1. INTRODUCTION

In general, the Critical Dimension [CD] variation is given as  $\pm 10\%$  of the minimum feature size. Therefore, for leading edge 248nm lithography this gives a budget after lithography of only 50nm. Small changes in resist thickness due to underlying topography can lead to thin film interference e.g. at i-line, a 54nm change in resist thickness [corresponding to a quarter wavelength]. It leads to approximately a 35% change in the energy required to clear a typical resist. This problem is even more severe at DUV where the reflectivity of the substrate is higher and the resist thickness is lower [1]. A number of methods have been proposed to address these TFI exposure variations [2-4] Initial work by Brewer et al [5] investigated polymers to absorb light penetrating through the photoresist thus eliminating standing waves. The basis of pattern transfer and optical properties of the polymer give rise to the foundation of BARC used on reflective substrates [6,7]. This concept was taken further and first applied to implementing BARC on device structures for enhanced linewidth control over topography by Y.C.Lin [8].

Standing wave phenomenon is described as the light-energy coupling variations through periodic minima and maxima corresponding to the destructive and constructive interference caused by the resist thickness variation. Increasing the thickness of resist can reduce the relative variations of the coupled energy so that there may be a decrease in the linewidth variation but this thickness increase may degrade the pattern transfer along with loss of depth of focus for high resolution applications. One of the first simulation tools employed to predict the vertical min-max separation was SAMPLE from Berkley [9], later more advanced simulation tools such as PROLITH™ [10] were introduced. Before discussing the merits of bottom anti-

reflective coatings, a brief overview of the theory associated with reflectivity control will be given. This leads to a section on top anti-reflective layers. However for the scope of this article this is only included for completeness.

## 2. THEORY

Multiple path length interference between the forward wave, the reflected wave from the substrate and that reflected from the air/resist interface give rise to an interference within the resist film, shown in figure 1. Changes in the path length, and therefore the incoupling into the resist vary. These variations are resist absorbed energy and are characterized by swing effects shown in Figure 2. This shows the periodic swing from a maximum dose to clear [destructive interference within the film or incoupling minimum] to a minimum dose to clear [constructive interference within the resist film or Maximum incoupling] as a function of resist thickness. Figure 3 shows the different contributions from resist thickness variation and also reflective notching and standing waves from reflective substrates.

The swing effect can be attributed to different resist thickness, or thickness variation of the transparent underlayer [oxide or nitride] resulting in different absorbing energies. The swing ratio is defined as

$$S=4(R_{top}R_{bot})^{0.5}.e^{-\alpha D}$$

where  $R_{top}$  is the reflectivity of the resist/air interface,  $R_{bot}$  is the reflectivity of the resist/substrate interface;  $\alpha$  is the resist absorption coefficient [the sum of standard Dill A and B parameters] and D is the resist thickness [11]

The intensity of light, which is reflected, depends on the absorbance of the resist, the reflectivity of the substrate and the local topography. To reduce the reflectivity from substrate one possibility currently used within the industry is the implementation of a dyed resist. Unfortunately, for small feature sizes in the micron- and sub-micron region, the use of dyed resists is unacceptable, due to deteriorated resist profiles, the unacceptable focus-exposure process window for minimal CD dispersion and the risk of resist residues between narrow spacing after pattern development. An alternative method for minimizing reflections is the use of top and bottom anti-reflective coating in conjunction with a resist of higher contrast.

### 2.1. Top Anti-reflective layer

Top Anti-reflective [TAR] coatings are applied on top of the photoresist shown in Figure 4. The TAR effects beams D, E, F and G in a way that beams D and G interfere destructively. For total destructive interference to occur the intensity has to be identical and therefore the refractive

index of the resist has to be the square root of the refractive index of the TAR.

$$n_{TAR}=[n_{resist}]^{0.5}$$

This yields an optimum TAR refractive index at i-line of 1.28. In addition, the phase of the two beams needs to be opposite; therefore the TAR thickness has to be quarter wavelength within the TAR. By monitoring the response of the CD variation as a function of TAR thickness it is possible to minimize the CD variation due to swing to near zero. Typical Commercial TAR have a refractive index near 1.4 [12].

### 2.2. Bottom Anti-reflective Coatings.

The variation of energy interacting with the resist is a function of the resist thickness and substrate reflectivity. By evaluating the contribution of the optical constants (n-ik) from both resist and BARC and also the thickness of BARC ( $T_b$ ), the substrate reflectivity curve from the BARC is a combination of three components [13]. Firstly as a result of the absorption from the BARC, the first component exponentially decreases at twice the thickness of BARC [as the light passes through the BARC twice; once into and once back from the substrate]:

$$R_1 \sim \exp(-2k_b T_b)$$

The second contribution is a periodic function due to interference effects within the BARC film, where the period is a function of the real component of the refractive index and the amplitude is related to the energy absorbed within the BARC film:

$$R_2 \sim \exp(-2k_b T_b) \sin(4\pi n_b T_b / (\lambda + \phi))$$

Thirdly, there is a background component, which never penetrates into the BARC based on the difference in refractive index between the resist and the BARC. This component is independent of the BARC thickness.

$$R_3 = \frac{(n_b - n_r)^2 + (k_b - k_r)^2}{(n_b + n_r)^2 + (k_b + k_r)^2}$$

It can be shown that if the absorbance of the BARC [ $k_b$ ] increases, this will cause a decrease in the reflectivity  $R_1$  and a small amplitude in the periodic oscillation  $R_2$ . But if the difference between the resist and BARC refractive index increases,  $R_3$  will increase and therefore the background reflectance will increase, resulting in a scenario very similar to if the BARC was metallic. The Superposition of all three components is represented in Figure 5.

## 3. BARC DESIGN REQUIREMENT

Two types of BARC have been identified [14]; Type I refer to Index matched [both real and imaginary] to the

photoresist, but are slightly more absorptive and are thick enough to suppress the reflectivity from the BARC/substrate interface. Type II BARCs rely on precise control of thickness since their basic mechanism is through interference and absorbance.

The implementation of these Chemical Vapor Deposited [CVD] Anti-reflective layers comprising Titanium Nitride, Silicon Nitride, Silicon Oxynitride and amorphous carbon have previously been reported [15,16]. As some of these systems are optically tunable, they have the potential of eliminating standing waves. However, as they are conformally deposited they do nothing to suppress the bulk effect within the planarizing resist film. Furthermore, CVD BARCs pose an integration challenge since the film must be electrically compatible with the overall process or completely removable via the etch step [15]. Such stripping and potential life-time failures are great concerns in the overall cost of ownership of the inorganic BARC process and will not be discussed further in this article.

Organic BARC materials can be categorized in terms of the wavelength of optimum absorbance and patterning mode. As was mentioned above, introducing an optimized organic BARC into the lithographic process can diminish standing waves, minimize resist notching and reduce CD swing.

Because the application of organic BARC is a spin on process generally the organic BARC is a liquid formulation consisting of the following main components: A polymer binder, a light absorbing material and a solvent system. Polymers designed for BARC coatings must have sufficient solubility in the formulation, be thermally stable, have good adhesion to the substrate, be inert to the solvent in the BARC formulation and also to the subsequent processing solvents and exhibit a high plasma etch rate. The light absorbing material must bear high or optimized absorbability for the given wavelength, high etch rate, inert to both BARC, resist and subsequent processing solvents and low or no sublimation. The solvent system must be environmentally safe, inert to the coating system and have a high flash point.

Several BARC systems have been developed at Brewer Science to date. These are Polymer-dye blending system, dye attached polymer systems, crosslinked polymer systems and thermal plastic polymer systems. Both wet-etchable and dry-etchable BARCs have been introduced to the market to meet customers' different needs. We will discuss more detailed BARC chemistries in a later paper.

#### 4. BARC OPTIMIZATION

As the high resolution photoresists are designed, the chemical matching between BARC and resist is more and more critical. At i-line, since chemically amplified and negative acting photoresists are still rare, little or no interfacial mixing has been observed with a typical BARC

such as Brewer Science' ARC@-XHRi. Current resist processes at i-line have demonstrated resolution down to 0.20 $\mu$ m with optical enhancement techniques shown in Figure 6. With all testing experiments, the demonstration of resolution capability on flat wafers is entirely different from sustaining a successful manufacturing process.

In order to obtain the optimum process, some or all of the following issues should be investigated:

- BARC Thickness
- BARC Bake temperature
- BARC breakthrough etch
- Optical feedback.

Figure 7 shows the impact of BARC on reducing thin film interference. The 110nm XHRi reflectivity maxima gives about a 6% reflectivity, while at 165nm a reflectivity minima gives nearly 0% reflectivity. In Figure 8, the CD variation caused by resist thickness from a TFI max to a TFI min, about 50nm, is shown.

#### 5. CONCLUSIONS

It has been the intention of this article to bring to light some of the possible benefits from the inclusion of a Bottom Anti-reflective coating process into manufacturing line, and highlight the benefits when weighed against the additional cost of ownership. Since BARCs are classified into families dependent on the illumination they are designed to work with, and the mode of pattern transfer through the BARC, we shall conclude with the applications and areas of optimization associated with each wavelength.

For broad-band and g-line manufacturing employ Brewer's polyamic acid ARC@-XLT primarily for metal etch applications. As feature sizes are generally larger than 0.8 $\mu$ m, bake windows for a sustainable manufacturing process are approximately 5-15 $^{\circ}$ C for a 0.8 to 1.2 $\mu$ m metal etch process in wet patterning mode. For dry patterning [requiring a BARC break through etch] the BARC is baked at 210 $^{\circ}$ C.

For resolution below 0.6 $\mu$ m, i-line is generally employed due to the spectral bandwidth encountered above 365nm. Here the wet patterning BARC WiDE™ is employed for intermediate structures of 0.6 to 0.4 $\mu$ m metal; front-end emitter and poly applications. Also, the dry patterning BARC XHRi for high-resolution front-end applications is an option. The mode of patterning has been shown to provide an additional tool for optimization. Wet patterning can be reworked easily and gives fast feedback on microscopic issues such as reflective notching during after develop inspect. Dry patterning gives the opportunity to tune the photo and bark break-through etch to compensate for etch bias during the substrate etch. In addition, the

ability to cover high topography [ $>0.7\mu\text{m}$ ] front-end flash and BiCMOS devices with a highly conformal i-line BARC is now available.

At DUV, BARC is required on more levels due to the increase in reflectivity from the substrate and the tighter CD dispersion requirements. As high resolution is required where developer transport can be limited by capillary effects, only dry patterning [plasma etched] BARCs are employed. Here more attention is required for matching between the DUV resists and BARC to ensure large focus and exposure latitude. Careful consideration of the reflectivity interference from the substrate is needed to ensure the reflectivity envelopes from the different thickness' of e.g. Oxide are controlled to sustain the litho process.

Future developments of lithography will introduce processes at 193nm exposure wavelength. This has not been covered within the article, as resist technology is still relatively immature. However, work is ongoing to optimize the BARC chemistry for resist compatibility.

## 6 REFERENCES

1. S.S.Miura, C.F.Lyons, T.A. Brunner, Proc SPIE 1674, 147, 1992
2. B. J. Lin, T.J.P. Chang, J. Vac-Science Technology 16, 1669, 1979.
3. C.H.Ting, K.L.Liau, Semiconductor International, p102, 1984
4. C.H.Ting, K.L.Liau, SPIE IEEE VLSI multilevel interconnect, 1984
5. T. Brewer, R Carlson and J. Arnold, J. Appl. Photogr. Eng. 7, 184, 1981.
6. R.D.Coyne, T. Brewer, Kodak Microelectronics, 40, 1983.
7. Arnold and Brewer, US Patent 4,910,122
8. Y.C. Lin, A.J.Purdes, S.A.Saller, W.R.Hunter, J.appl.Phys, 55, 4, 1110, 1984.
9. W.G.Oldham, G.Nandgaonhar, A.R.Neureuther and M.O'Toole, IEEE Trans., ED 26, 717, 1979.
10. PROLITH is a registered trademark of Finle Technologies.
11. T. Brunner, Proc SPIE 1466, 297, 1991
12. Technical data for NFC600 from JSR and for AquaTar from AZ-Clariant
13. Maaik Op de Beeck et al, Future Fab International Vol. 5, Pg 205
14. H. Dijkstra, C Juffermans, SPIE 1927, 275, 1993
15. Y.Tani et al. Jpn. J. Appl. Phys., 32, 5909, 1993
16. T Gocho et. al. Jpn. J. Appl Phys., 33 486 1994
17. J. Sturtevant, M. Chara et.at. SPIE 2440, 582, 1995.

## 7 ACKNOWLEDGEMENTS

The authors would like to thank Jim Lamb for technical consultants and Bill Simmons for his simulation work.

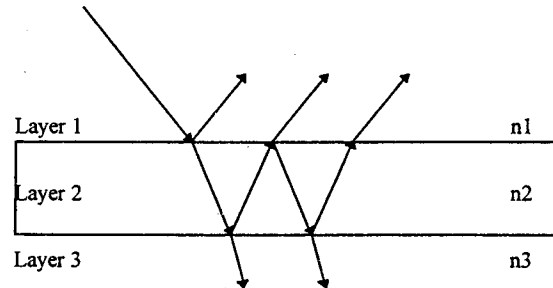


Fig. 1 Geometry showing reflections from and within a thin layer of resist [oblique angles used for illustration], within photolithography, the illumination is generally at normal incidence]

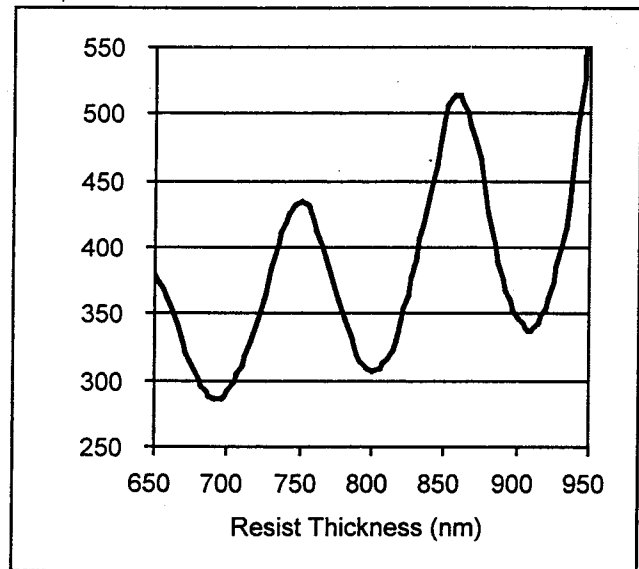


Fig. 2 Simulation demonstrating the thin film effect known as "Swing Curve"

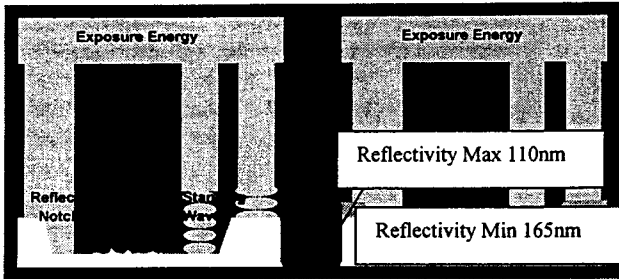


Fig. 4 Schematic diagram representing optical scheme of incident light into photoresist through TA between BARC and resist.

Fig. 3 Graphic representing some of the benefits of introducing a bottom Anti-reflective coating, highlighting standing waves, topography effects like reflective notching and thin film interference.

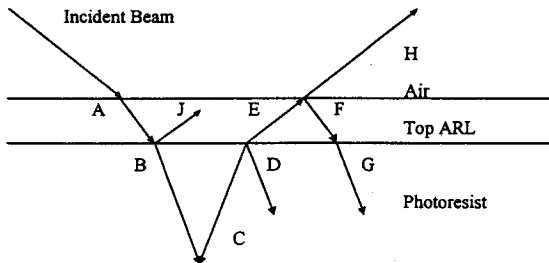
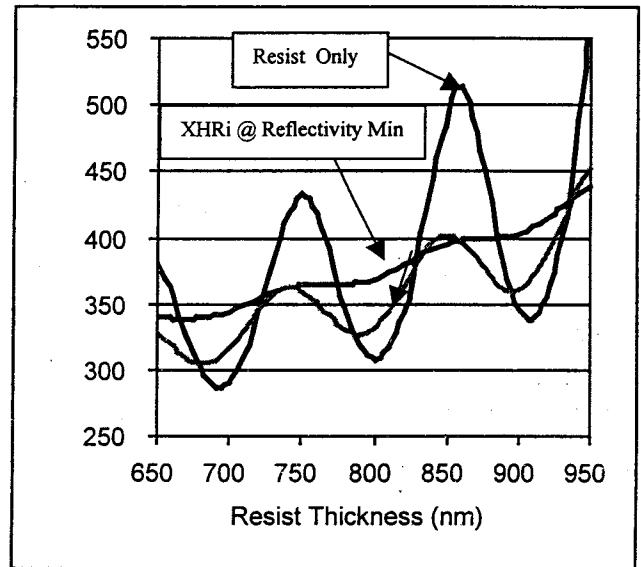
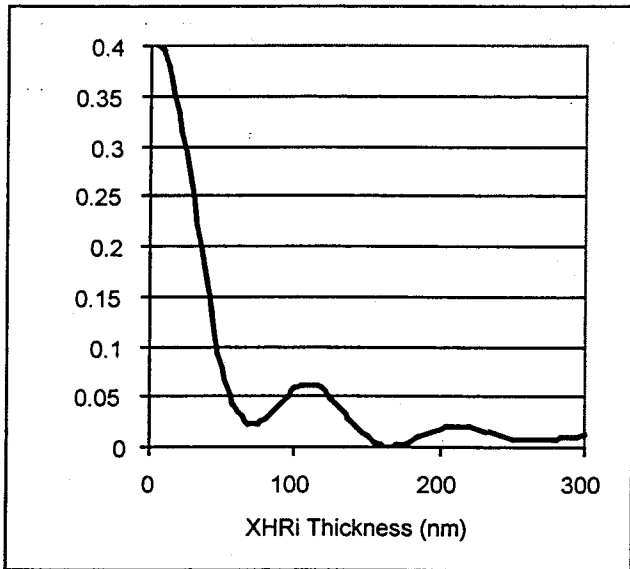


Fig. 5 Simulation of the three reflectivity components which contribute to the total reflectivity between BARC and resist.

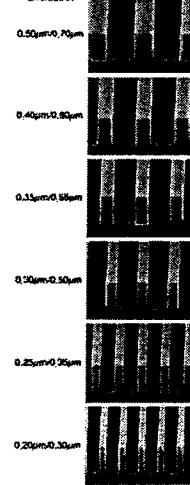


**JSR**  
FLUOROCHEM

**IX1070G, 16cP**  
on BARC

**Line & Space Resolution**  
Energy: 200mJ/cm<sup>2</sup>  
Defocus: ±0.0μm

Resolution



**Process Conditions**  
Substrate: Poly Silicon  
BARC: 180nm XHRi  
Thickness: 6.77nm (E<sub>max</sub>)  
Spin Rate: 500 RPM  
Exposure: 230mJ/cm<sup>2</sup>  
NA = 0.57 σ = 0.67  
Energy = 200mJ/cm<sup>2</sup>  
Defocus = ±0.0μm  
110°C 20s  
Development: 0.30N TMAH  
See Single Puller

TRF 2214

Fig. 6 Resolution currently available from JSR IX1070 a leading i-line resist [Data presented from JSR].

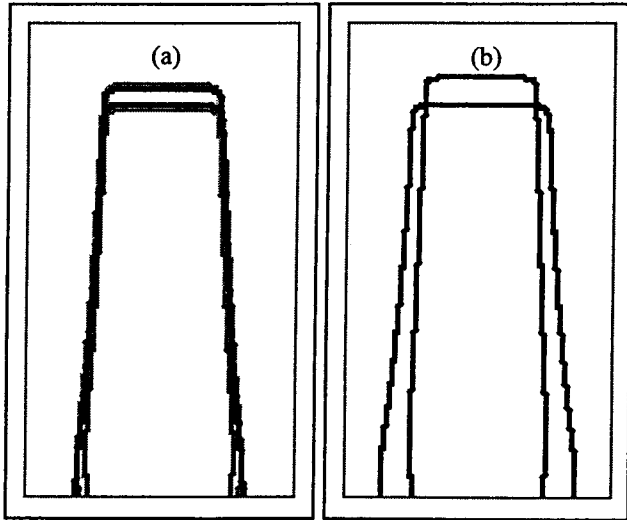


Fig 8 Profile variation for  $0.35\mu\text{m}$  lines with resist thickness change from standing wave minima to standing wave maxima. (a) With XHRi at reflectivity minima and maxima, (b) without BARC.

For further information, please contact  
Mr. Paul Williams at 573-364-0300 or [pwilliams@brewerscience.com](mailto:pwilliams@brewerscience.com)